

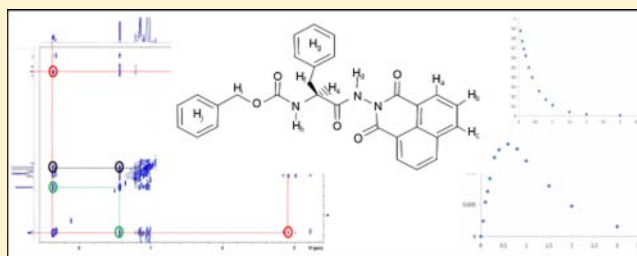
# New Application of Proton Nuclear Spin Relaxation Unraveling the Intermolecular Structural Features of Low-Molecular-Weight Organogel Fibers

Sabine Bouguet-Bonnet, Mehdi Yemloul, and Daniel Canet\*

Méthodologie RMN (CRM<sup>2</sup>, UMR 7036, UL-CNRS), Université de Lorraine, Campus Aiguillettes, B.P. 70239, 54506 Vandœuvre-lès-Nancy (cedex), France

**S** Supporting Information

**ABSTRACT:** Proton nuclear spin relaxation has been for the first time extensively used for a structural and dynamical study of low-molecular-weight organogels. The gelator in the present study is a modified phenylalanine amino acid bearing a naphthalimide moiety. From  $T_1$  (spin–lattice relaxation time in the laboratory frame) and  $T_{1\rho}$  (spin–lattice relaxation time in the rotating frame) measurements, it is shown that the visible gelator NMR spectrum below the liquid–gel transition temperature corresponds to a so-called isotropic compartment, where gelator molecules behave as in a liquid phase but exchange rapidly with the molecules constituting the gel structure. This feature allows one to derive, from accessible parameters, information about the gel itself. Nuclear Overhauser effect spectroscopy (NOESY) experiments have been exploited in view of determining not only cross-relaxation rates but also specific longitudinal rates. The whole set of relaxation parameters (at 25 °C) leads to a correlation time of 5 ns for gelator molecules within the gel structure and 150 ps for gelator molecules in the isotropic phase. This confirms, on one hand, the flexibility of the organogel fibers and, on the other hand, the likely presence of clusters in the isotropic phase. Concerning cross-relaxation rates, a thorough theoretical investigation in multispin systems of direct and relayed correlations in a NOESY spectrum allows one to make conclusions about contacts (around 2–3 Å) not only between naphthalimide moieties of different gelator molecules but also between the phenyl ring and the naphthalimide moiety again of different gelator molecules. As a result, not only is the head-to-tail structure of amino acid columns confirmed but also the entangling of nearby columns by the naphthalimide moieties is demonstrated.



## INTRODUCTION

Organogels are generally formed by self-aggregation of gelators, leading to the formation of fibrous three-dimensional networks with cross-links among the nanofibers possibly entrapping the solvent.<sup>1–4</sup> Due to present and potential applications, organogels have attracted much interest. Various molecules are prone to form an organogel in an appropriate solvent, and recently, a new class of strong low-molecular-weight organogelators, based on amino acid derivatives, have come out.<sup>5,6</sup> In the fibers, gelator molecules are assembled through gelator–gelator interactions involving noncovalent bonding (H-bonding, van der Waals,  $\pi$ -stacking, ...) with a strong self-complementarity and unidirectional intermolecular cohesion.

The system we are interested in involves as the gelator an amino acid (phenylalanine) modified with a naphthalimide moiety prone to form a gel in an appropriate solvent (here toluene). After having demonstrated the passivity of the solvent once the organogel is formed,<sup>7</sup> we address the issue of the gel structure. A first NOESY (nuclear Overhauser effect spectroscopy) determination<sup>8</sup> showed that  $\pi$ – $\pi$  stacking was responsible for a head-to-tail arrangement of gelator columns constituting the basic building block of the organogel structure. The present study is aimed at going deeply into the dynamics

and structure of the fibers constituting the organogel, and we shall see that proton nuclear spin relaxation is the proper tool for directly accessing the relevant information. We shall start with a series of proton spin–lattice relaxation (in the laboratory frame and in the rotating frame) measurements as a function of temperature (i.e., in the gel phase and in the liquid phase) to get some insight into the gelator dynamical properties. It turns out that one observes a high-resolution spectrum of the gelator below the liquid–gel transition temperature which is attributable to the gelator molecules within the so-called isotropic phase (liquid phase). The latter coexists with the gel structure. Moreover, these relaxation times demonstrate that gelator molecules in the isotropic phase and in the gel structure exchange rapidly. Although the gelator molecules within the gel phase do not lead to an observable spectrum (due to strong dipolar interactions which produce an important line broadening), the key feature is that this exchange phenomenon will allow us to measure indirectly the relaxation parameters of gelator molecules within the gel structure. Thereafter, we have turned to two-dimensional NOESY spectra to demonstrate and

Received: April 17, 2012

Published: June 4, 2012

confirm the organogel structure, noticeably by looking at possible entangling of gelator columns. This has required a deep analysis of NOESY spectra as a function of the so-called mixing time (the interval during which nuclear spins interchange energy, thus revealing correlations through dipolar interactions). Indeed, NOESY experiments have proved invaluable in structural determinations, noticeably for large biomolecules. This is because slow tumbling motions entail intense NOESY cross-peaks. In the past, one relied on a semiquantitative treatment based on the cross-peak intensities (high, medium, or low).<sup>9,10</sup> As we are dealing here with a system which also involves slow tumbling (thus relatively intense cross-peaks) and because the gelator is a medium-size molecule (with a limited number of visible cross-peaks), we can hope to derive quantitative information from the evolution of the cross-peak intensities as a function of the mixing time. In particular, it will be recalled that the initial behavior (short mixing times) can unravel direct or relayed dipolar interactions capable of providing reliable information about the organogel structure. It can be mentioned that, even in the case of large biomolecules, the present tendency is to use NOESY data more quantitatively.

## EXPERIMENTAL SECTION

The organogelator (see Figure 1) was synthesized according to procedures described previously.<sup>6</sup> It was dissolved in perdeuterated toluene at 0.5 wt % so that the gel–liquid transition occurs around 50 °C. The sample was inserted into a classical 5 mm o.d. sample tube which was subsequently sealed.

Proton spin–lattice relaxation times in the laboratory frame ( $T_1$ ) and in the rotating frame ( $T_{1\rho}$ ) were measured between 10 and 90 °C with a Bruker spectrometer operating at 400 MHz (Nancy). The former were obtained through the classical inversion–recovery method. For the latter, spin-lock periods of appropriate durations were employed with a relatively small radio frequency field amplitude ( $\gamma B_1/2\pi = 1000$  Hz) to prevent probe damage. For avoiding off-resonance effects, it was found necessary to perform several separate measurements with the carrier frequency close to the resonance frequency of the considered proton.

For rotating-frame relaxation dispersion experiments, which consist of measuring  $R_{1\rho}$  ( $R_{1\rho} = 1/T_{1\rho}$ ) as a function of the radio frequency field amplitude, a homemade 200 MHz spectrometer equipped with a dedicated probe<sup>11</sup> (for accommodating large rf field amplitudes) was employed.

NOESY and  $T_1$  experiments were performed according to the standard sequences at 25 °C (gel phase) with Bruker instruments operating at 300 and 600 MHz (Nancy) and 800 and 1000 MHz (Lyon).

## PROTON SPIN–LATTICE (LABORATORY-FRAME AND ROTATING-FRAME) RELAXATION OF THE ORGANOGEATOR

Proton NMR spectra (a) at a temperature where the organogel is present and (b) above the gel–liquid transition are shown in Figure 1. Besides some chemical shift modifications which demonstrate that interactions experienced by the gelator molecules are different in the two phases, one observes that a high-resolution spectrum remains when the organogel is present. However, its intensity is much lower than in the liquid phase, beyond the gel–liquid transition, indicating that the gelator molecules involved in the organogel structure are, as expected (due to its solid-state character and to large dipolar interactions), NMR silent. In fact, in these systems, it is well-known<sup>12</sup> that the organogel formation does not require the totality of the gelator molecules (in the following,  $p$  will denote

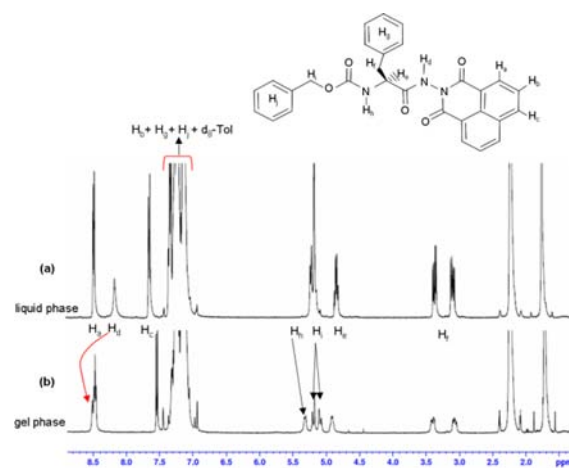


**Figure 1.** Proton NMR (400 MHz) spectra of the molecule shown in the inset (0.5% in toluene- $d_8$ ): (a) liquid phase at 70 °C, (b) gel phase at 15 °C.

the proportion of gelator molecules entering the gel structure). The rest (about 70% in our case at 25 °C;  $p = 0.3$ ) is said to be in the isotropic phase, in other words, in the solvent phase. As will be seen later, gelator molecules in the isotropic phase apparently undergo slow motions which cannot take place in a liquid phase for such a medium-size molecule. Owing to the flexibility of the gel fibers, one can envision a fast exchange process between gelator molecules in the gel phase and in the isotropic phase. In this way, as molecules giving rise to the visible NMR spectrum spend some time within the gel, they bear information about the dynamics and structure of the gel fibers. Such a situation has been frequently exploited in the case of fast exchange between free ligands bound to a macromolecular entity.<sup>13,14</sup>

We have previously shown that, once the organogel is formed, the solvent is passive.<sup>7</sup> In this paper, with the objective to obtain some information about the organogel, we shall first ascertain that fast exchange between the gel structure and the isotropic phase really takes place. For that purpose, we have carried out some measurements of proton nuclear relaxation times in a temperature range (10–90 °C) including the gel–liquid transition. They of course include the longitudinal relaxation time  $T_1$ , but because of the echo amplitude modulation due to  $J$  couplings (we are dealing here with a proton spectrum involving many multiplets), it proved impossible to measure the transverse relaxation time  $T_2$  by conventional methods based on spin echoes. An alternative is the so-called relaxation time in the rotating frame,  $T_{1\rho}$ , which is known to carry the same (or similar) information as  $T_2$ . It is measured from the decay of nuclear magnetization locked by the radio frequency field (the alternating magnetic field used in NMR for manipulating nuclear magnetization), and as nuclear magnetization is not allowed to precess,  $J$  modulation cannot occur. In fact, the comparison of  $T_1$  and  $T_2$  (in our case  $T_{1\rho}$ ) can reveal slow reorientational motions or exchange phenomena. In the absence of these two features (one or the other), the so-called extreme narrowing conditions prevail ( $\omega\tau_c \ll 1$ ; see eq 1):  $T_{1\rho} = T_1$ .

For the system under investigation, we can safely consider only two relaxation mechanisms: dipolar interactions and, possibly, chemical exchange which is known to affect  $T_{1\rho}$  and not  $T_1$ . In a general way, inverses of relaxation times (called

relaxation rates) can be expressed as a function of spectral densities. The simplest form for the latter is

$$\tilde{J}(\omega) = \frac{2\tau_c}{1 + \omega^2\tau_c^2} \quad (1)$$

where the correlation time  $\tau_c$  is characteristic of the considered motion and  $\omega$  a frequency ( $\text{rad s}^{-1}$ ).

The major differences between  $T_1$  and  $T_{1\rho}$  are (i) the presence in  $R_{1\rho}(1/T_{1\rho})$  of a spectral density at zero frequency in addition to spectral densities at the measurement frequency (and twice this measurement frequency) solely involved in  $R_1(1/T_1)$  and (ii) exchange (chemical, conformational, or between different sites) which affects only  $T_{1\rho}$ . When slow motions occur, the spectral density at zero frequency becomes predominant so that  $T_{1\rho}$  becomes shorter than  $T_1$ . Conversely, in the absence of slow motions (extreme narrowing) or exchange,  $T_{1\rho} = T_1$ . We present now two typical results along with a qualitative interpretation. Proton  $H_a$  is typical in the sense that it cannot be subjected to chemical exchange and that it belongs to a rigid part of the molecule, thus essentially affected by overall tumbling. The evolution of the two relaxation times with temperature is displayed in Figure 2. It

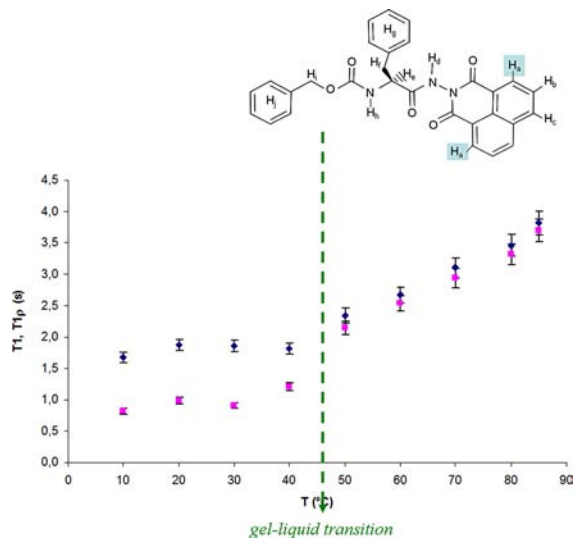


**Figure 2.** Evolution of  $T_1$  (circles) and  $T_{1\rho}$  (squares) of the  $H_a$  proton as a function of temperature. Measurements were performed at 400 MHz.

can be seen that in the gel phase  $T_{1\rho}$  is roughly 2 times smaller than  $T_1$ . As explained above, this is due to the contribution of the slow motions taking place within the organogel structure and possibly to exchange phenomena. Above the gel–liquid transition both relaxation times become identical, confirming that extreme narrowing conditions are reached and that any slow motion has disappeared. The evolution of relaxation times with temperature confirms also that gelator molecules in the isotropic phase carry information about the organogel structure.

Results pertaining to proton  $H_d$  are displayed in Figure 3. The evolution of  $T_1$  is as expected and comparable to what is observed for  $H_a$ . However, the behavior of  $T_{1\rho}$  is quite different, revealing a significant contribution from exchange phenomena. This is not surprising for this amide proton, due to its possible labile character. It is very likely that the exchange contribution is overwhelming since (i) one does not observe any significant variation at the gel–liquid transition and (ii) contrary to what

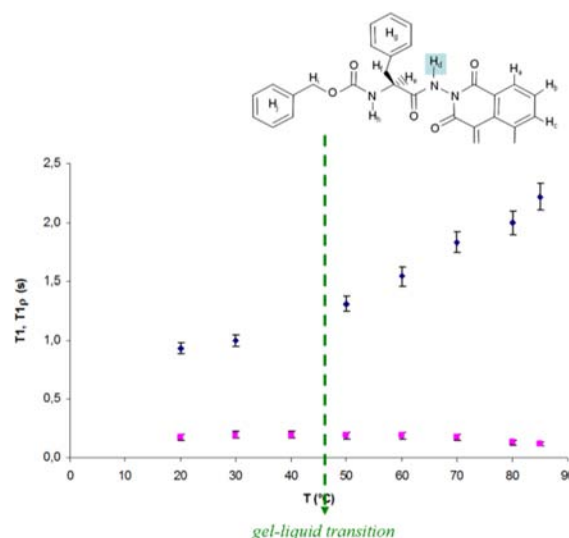


**Figure 3.** Evolution of  $T_1$  (circles) and  $T_{1\rho}$  (squares) of the  $H_d$  proton as a function of temperature. Measurements were performed at 400 MHz.

occurs with most relaxation mechanisms (e.g., dipolar interactions), one observes a decrease of  $T_{1\rho}$  when the temperature increases. In fact, this feature can be easily explained by the expected acceleration of exchange. Protons  $H_a$  and  $H_d$  represent two extreme situations, the former being only subjected to dipolar relaxation mechanisms which, for the latter, add to a strong exchange contribution affecting only  $T_{1\rho}$ . Results obtained for other protons in the gelator molecule (not shown) can be interpreted according to the relative importance of these two contributions.

To confirm or to complement the above findings, we have carried out  $T_{1\rho}$  measurements as a function of the radio-frequency (rf) field amplitude. This latter quantity, expressed as  $\omega_1 = \gamma B_1$  ( $\gamma$  is the gyromagnetic ratio), allows us to probe  $T_{1\rho}$  as a function of  $\omega_1$ , thus possibly revealing different dynamical regimes. This approach is widely used in the study of proteins and generally yields information about exchange phenomena.<sup>15–17</sup> Experimental results are generally presented as dispersion curves  $R_{1\rho}(1/T_{1\rho})$  vs  $\omega_1$ . Data shown in Figures 4 and 5 correspond, for protons  $H_a$  and  $H_b$  to the gel phase (20 °C) and to the liquid phase (70 °C), above the gel–liquid transition.

Dispersion curves have been analyzed as one or two (superposed) Lorentzian function(s). It can be seen that, for  $H_a$ ,  $R_{1\rho}$  is independent of  $\omega_1$  at high temperature, meaning that this proton, in the liquid phase, is not subjected to any exchange phenomenon. Conversely, its evolution in the gel phase (20 °C) is indicative of an exchange process, the only possibility being an exchange between the gel structure and the isotropic phase. In that case,  $R_{1\rho}$  can be expressed as<sup>18,19</sup>

$$R_{1\rho} = (\delta\omega)^2 p(1-p) \frac{\tau_{\text{ex}}}{1 + \omega_1^2 \tau_{\text{ex}}^2} + R_{1\rho}^0 \quad (2)$$

$\delta\omega$  is the chemical shift difference between the two sites,  $p$  is the proportion of the gelator constituting the gel structure, and  $\tau_{\text{ex}}$  is the exchange characteristic time (the inverse of the exchange rate).  $R_{1\rho}^0$  encompasses all nonexchange contributions. Of course,  $\tau_{\text{ex}}$  and  $R_{1\rho}^0$  will be deduced from the variation of  $R_{1\rho}$  with  $\omega_1$ . As  $p$  is known (see above),  $\delta\omega$  can also be extracted from the analysis of these dispersion curves.

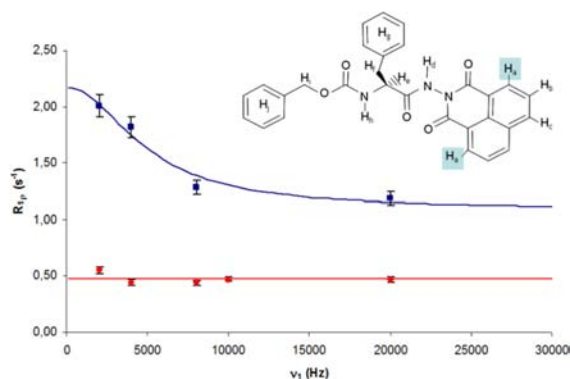


**Figure 4.** Evolution of the  $H_a$  rotating-frame relaxation rate ( $R_{1\rho}$ ) as a function of the radio-frequency field amplitude  $B_1$  ( $\nu_1 = \omega_1/2\pi = \gamma B_1/2\pi$ ): squares, 20 °C (gel phase); circles, 70 °C (liquid phase); solid lines, curves recalculated according to eq 2 and from parameters given in Table 1.

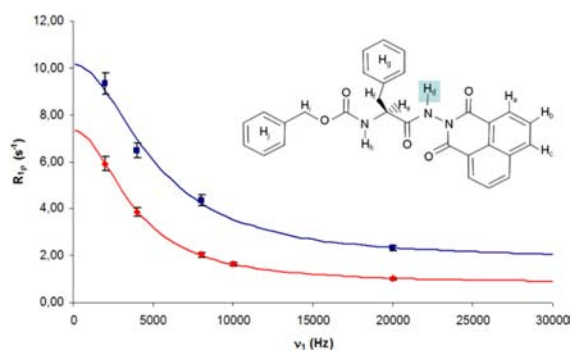


**Figure 5.** Evolution of the  $H_d$  rotating-frame relaxation rate ( $R_{1\rho}$ ) as a function of the radio-frequency field amplitude  $B_1$  ( $\nu_1 = \omega_1/2\pi = \gamma B_1/2\pi$ ): squares, 20 °C (gel phase); circles, 70 °C (liquid phase); solid lines, curves recalculated according to eq 2 and from parameters given in Table 1.

On the other hand, when chemical exchange is present (proton  $H_d$ ; see above), this is reflected by a variation of  $R_{1\rho}$  with  $\omega_1$  at high temperature which can be analyzed with an equation similar to eq 2 (the only difference comes from the factor  $(\delta\omega)^2 p(1-p)$  which has been contracted in a single constant). Conversely, in the gel phase (low temperature), we must, in addition, take into account the exchange between the two sites (gel structure–isotropic phase). This implies that experimental data must be fitted according to the superposition of two Lorentzian functions. Recalculated curves as well as parameters are given in Figures 4 and 5 and Table 1.

**Table 1. Parameters Used for the Recalculated Curves Shown in Figures 4 and 5<sup>a</sup>**

	$H_a$	$H_d$
$\delta\omega$ at 20 °C (rad s <sup>-1</sup> )	385	1000
$p$ at 20 °C		0.35
$\tau_{ex}$ at 20 °C (10 <sup>-5</sup> s)		3.5
$\tau_{ex}'$ at 70 °C (10 <sup>-5</sup> s)		2.6
$R_{1\rho}^0$ at 20 °C (s <sup>-1</sup> )	1.09	1.83
$R_{1\rho}^0$ at 70 °C (s <sup>-1</sup> )	0.48	0.81

<sup>a</sup> $\tau_{ex}$  = exchange between the gel structure and isotropic phase, and  $\tau_{ex}'$  = chemical exchange.

The essential point, which confirms the validity of the present approach, is the similarity of the values found for the exchange rate between the gel structure and the isotropic phase (around  $3 \times 10^{-5}$  s). This value corroborates the validity of the fast exchange hypothesis for organogelator molecules within the so-called isotropic phase and organogelator molecules participating in the gel structure (exchange would be slow if the difference in resonance frequency were greater than 10 kHz, which obviously cannot be the case with proton spectra). Moreover, it appears clearly that the latter are subjected to slow motions which, unfortunately, cannot be fully characterized through a comparison between  $T_1$  and  $T_{1\rho}$  because exchange phenomena complicate the quantitative interpretation of rotating-frame spin–lattice relaxation data. Nevertheless, from this first approach, it is apparent that the visible proton NMR spectrum depends, thanks to a fast exchange regime, not only on the gelator molecules within the isotropic phase but also on molecules belonging to the gel structure. It can thus be hoped that NOESY experiments which depend solely on dipolar interactions can provide reliable information about the organogelator in the gel structure.

## NOESY EXPERIMENTS

First, let us recall the classical NOESY sequence

$$(\pi/2)_x - t_1 - (\pi/2)_x - t_m - (\pi/2) - \text{Acq}(t_2) \quad (3)$$

$(\pi/2)$  stands for a radio-frequency pulse,  $t_1$  and  $t_2$  are the time variables of the 2D experiment, and  $t_m$  is the so-called mixing time during which spins communicate by cross-relaxation. A typical NOESY diagram of the organogel phase is shown in Figure 6. Because some parts of the 1D spectrum are relatively

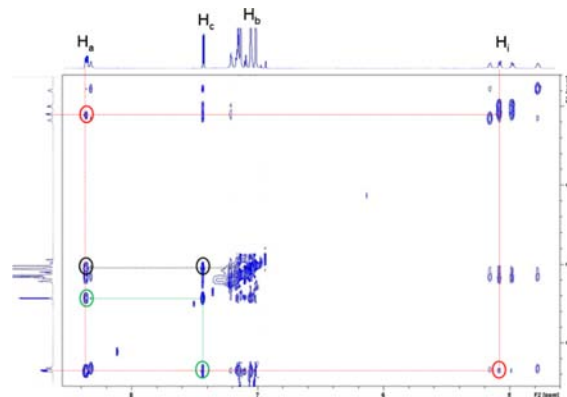


**Figure 6.** NOESY (1000 MHz) diagram of the organogel under investigation at 25 °C (mixing time 800 ms). Circles indicate the correlations which have been selected for measuring cross-relaxation rates.

crowded and because of the intense signals originating from toluene residual protons, there are only a few cross-peaks that can be really accessed. Furthermore, as explained in the Supporting Information, the corresponding diagonal peaks also have to be measured, still limiting further the number of correlations which can be reliably studied.

In a prospective way (we shall see later that it is the initial behavior which really matters), the whole buildup curves (cross-peak intensity as a function of the mixing time) corresponding to each considered cross-peak were obtained by means of separate experiments, each of them involving a different mixing time (Figure 7). Although they could be

generally fitted according to the equations of a two-spin system, we systematically relied on their initial behavior (see the Supporting Information).

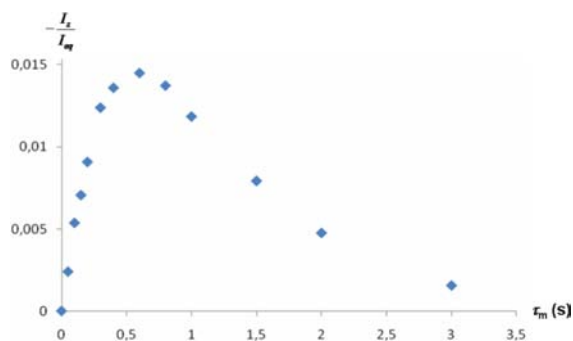


**Figure 7.** Typical NOESY buildup curve (here  $H_a-H_b$ ), normalized with respect to an appropriate equilibrium polarization (obtained from diagonal peaks at zero mixing time).

Finally, the decay curves of diagonal peaks (associated with the cross-peaks retained in this study) were obtained through the same set of experiments (Figure 8). They could be systematically fitted according to a monoexponential function which is believed to provide specific longitudinal relaxation rates. They have been compared to nonselective relaxation rates determined from classical inversion–recovery experiments.

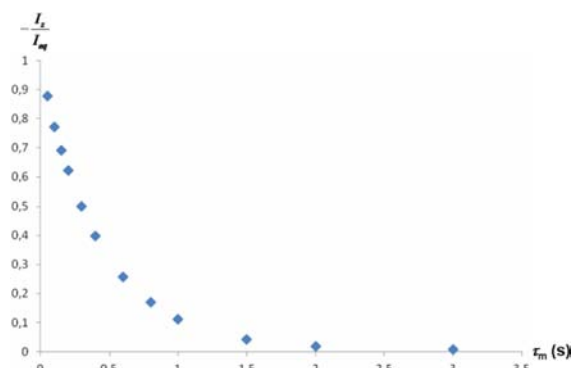


**Figure 8.** Typical decay (here  $H_a$ , normalized with respect to the intensity at zero mixing time) of a diagonal peak in a NOESY experiment demonstrating the possibility of measuring a specific longitudinal relaxation rate.

The interpretation of results arising from NOESY experiments rests on Solomon equations,<sup>20</sup> or rather extended Solomon equations in the case of a multispin system. It is recalled in the Supporting Information that, for a multispin system, reliable results can only be deduced from the initial behavior (short mixing times) either of cross-peak buildup curves or of diagonal peak decays. Thus, if we denote by  $s_{ij}$  the reduced intensity of the  $(ij)$  cross-peak (row corresponding to proton  $i$  and column corresponding to proton  $j$ ),  $s_{ij} = -E_{ij}/I_{eqj}$ ,  $E_{ij}$  being the actual cross-peak intensity and  $I_{eqj}$  the diagonal peak intensity corresponding to proton  $j$ . The latter is measured from the NOESY spectrum at zero mixing time. As shown in the Supporting Information, whatever the complexity of the spin system, we can write in the case of *direct* correlation between protons  $i$  and  $j$

$$s_{ij}(t_m) \approx -t_m \sigma_{ij} \quad (4)$$

In that case, the cross-relaxation rate is simply deduced from the initial slope in a  $t_m$  representation.

Consider now an  $(ij)$  cross-peak which is mediated by dipolar interactions with a third spin  $l$ :  $(i,l)$  and  $(l,j)$  interactions. Assuming that the direct  $(ij)$  dipolar interaction is negligible, we obtain for such a cross-peak (which will be dubbed “relayed” in the following)

$$s_{ij}(t_m) \approx \frac{t_m^2}{2} \sum_{l \neq i,j} \sigma_{il} \sigma_{lj} \quad (5)$$

This expression, derived in the Supporting Information, is in agreement with the literature<sup>21,22</sup>. The important point here is that a product of cross-relaxation rates is obtained from the initial slope in a  $t_m^2$  representation.

Finally, the initial behavior of the diagonal peak pertaining to proton  $i$  can be expressed as follows (still derived in the Supporting Information and with the notations of the precedent equations):

$$s_{ii}(t_m) \approx 1 - t_m R_i \quad (6)$$

The *specific* relaxation rate of proton  $i$ , denoted as  $(R_i^i)_{\text{diag}}$  in the following, can thus be derived from the initial slope of the relevant diagonal peak in a  $t_m$  representation.

## ■ DATA ANALYSIS

Our aim is now to determine molecular parameters from the whole set of data that we have at hand. Those molecular parameters we want to access are (i) the correlation times describing the molecular reorientation within the organogel structure, and possibly in the isotropic phase, and (ii) internuclear distances between the gelator molecules within the gel structure. To this end, we shall rest on theoretical expressions concerning the experimental parameters which can be reliably used. In this respect, relaxation rates in the rotating frame will be disregarded in this quantitative discussion because they entail an exchange contribution difficult to deal with (see above). In other words, we shall be dealing with (i) the classical longitudinal relaxation rate measured by a *nonselective* experiment (see the spin–lattice relaxation section), denoted below as  $(R_i^i)_{\text{IR}}$  (IR for inversion–recovery), (ii) the specific longitudinal relaxation rate  $(R_i^i)_{\text{diag}}$  measured from NOESY diagonal peaks, and (iii) cross-relaxation rates measured from NOESY cross-peaks.

**Correlation Times.** In a general way and in our situation of fast exchange between the isotropic phase and the gel structure (as demonstrated above), any relaxation parameter  $R$  can be written as

$$R_{\text{obsd}} = pR_{\text{gel}} + (1-p)R_{\text{iso}} \quad (7)$$

Remember that  $p$  is the proportion of the gelator molecules constituting the gel structure and is determined independently from spectral intensities (see above:  $p = 0.3$  at 25 °C). We now give handy expressions (derived from classical relaxation theory) for the various parameters which we shall be dealing with. In fact, we shall limit ourselves to relaxation of proton  $H_a$  because it belongs to the rigid part of the gelator molecule and because it can be anticipated that its relaxation is dominated by the  $H_a-H_b$  dipolar interaction. Thus, we can write

$$(R_1^{H_a})_{\text{IR}} = p(R_1^{H_a-H_b})_{\text{IR,gel}} + (1-p)(R_1^{H_a-H_b})_{\text{IR,iso}} + (R_1^{H_a})_{\text{IR,others}} \quad (8)$$

$$(R_1^{H_a})_{\text{diag}} = p(R_1^{H_a-H_b})_{\text{diag, gel}} + (1-p)(R_1^{H_a-H_b})_{\text{diag, iso}} + (R_1^{H_a})_{\text{diag, others}} \quad (9)$$

$$\sigma_{H_a-H_b} = p(\sigma_{ab})_{\text{gel}} + (1-p)(\sigma_{ab})_{\text{iso}} \quad (10)$$

In the above equations,  $R_1^{H_a-H_b}$  represents the  $H_a-H_b$  dipolar contribution to the relevant relaxation rate whereas  $(R_1^{H_a})_{\text{others}}$  stands for all other dipolar contributions. To handle the problem, we shall assume that these latter quantities (which could be considered as corrections) are frequency independent. We can write

$$(R_1^{H_a-H_b})_{\text{IR}} = K_d \left[ 3 \frac{2\tau_c}{1 + \omega_H^2 \tau_c^2} + 12 \frac{2\tau_c}{1 + 4\omega_H^2 \tau_c^2} \right] \quad (11)$$

$$(R_1^{H_a-H_b})_{\text{diag}} = K_d \left[ 3 \frac{2\tau_c}{1 + \omega_H^2 \tau_c^2} + 6 \frac{2\tau_c}{1 + 4\omega_H^2 \tau_c^2} + 2\tau_c \right] \quad (12)$$

$$\sigma_{ab} = K_d \left[ 6 \frac{2\tau_c}{1 + 4\omega_H^2 \tau_c^2} - 2\tau_c \right] \quad (13)$$

In these equations,  $K_d$  contains the usual constants (i.e.,  $(\mu_0/4\pi)^2 \hbar^2 \gamma_H^4$ ), with  $\mu_0$  the vacuum permeability,  $\hbar$  the Planck constant divided by  $2\pi$ , and  $\gamma_H$  the proton gyromagnetic ratio) and  $1/r_{ab}^6$  (here  $r_{ab}$  will be set to 2.5 Å), while  $\tau_c$  is the correlation time associated with the reorientation of the considered entity. Of course, we expect  $(\tau_c)_{\text{gel}} > (\tau_c)_{\text{iso}}$ .

Data at 300, 600, 800, and 1000 MHz are available. They have been fitted against  $(\tau_c)_{\text{gel}}$ ,  $(\tau_c)_{\text{iso}}$ ,  $(R_1^{H_a})_{\text{IR, others}}$ , and  $(R_1^{H_a})_{\text{diag, others}}$ . Experimental data along with recalculated curves are given in Figure 9. There is indeed an evolution with the

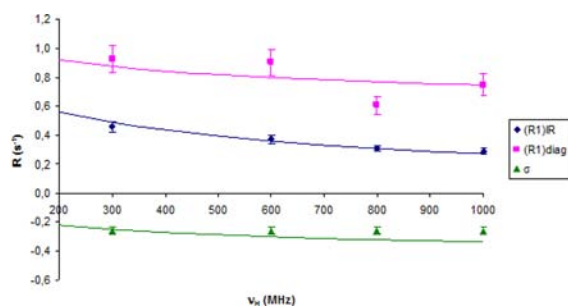


**Figure 9.** Proton  $H_a$  relaxation rates (squares,  $(R_1^{H_a})_{\text{IR}}$ ; circles,  $(R_1^{H_a})_{\text{diag}}$ ; triangles,  $\sigma_{H_a-H_b}$ ) at 25 °C as a function of the  $^1H$  measurement frequency; full curves, recalculated according to eqs 8–13 with  $(\tau_c)_{\text{gel}} = 5$  ns,  $(\tau_c)_{\text{iso}} = 150$  ps,  $(R_1^{H_a})_{\text{IR, others}} = 0.17$  s $^{-1}$ , and  $(R_1^{H_a})_{\text{diag, others}} = 0.31$  s $^{-1}$  (best fit of the experimental data).

measurement frequency which in turn allows us to obtain a proper estimation of the two correlation times. We find  $(\tau_c)_{\text{gel}} = 5$  ns and  $(\tau_c)_{\text{iso}} = 150$  ps.  $(\tau_c)_{\text{iso}}$  probably indicates that gelator molecules form small clusters at this temperature (the correlation time associated with the reorientation of a single molecule of a similar size is expected to be around 50 ps). Conversely,  $(\tau_c)_{\text{gel}}$  indicates that the gel structure is not very rigid. This is of course to be related to the fiber system which constitutes organogels.

**Structural Parameters.** We turn now to an analysis of cross-relaxation rates directed to geometrical determinations. As indicated above, the intensity of some cross-peaks can be

measured in good conditions, either from a two-spin analysis (checked by the corresponding initial slope) for direct correlations or from the initial slope in a  $t_m^2$  representation in the case of a relayed correlation. Indeed, the latter can be differentiated from the former by the initial behavior ( $t_m$  representation) as shown in Figure 10.

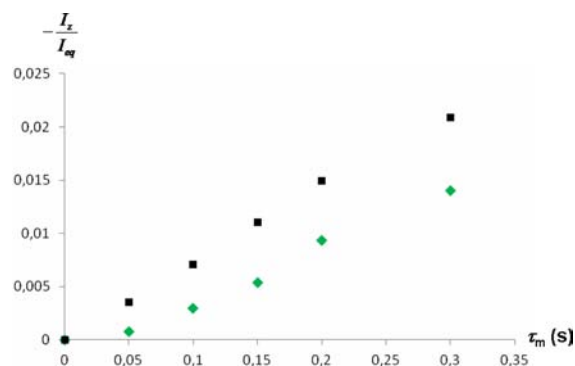


**Figure 10.** Two different initial behaviors of NOESY cross-peak intensities: linear behavior (squares), direct  $H_aH_c$  correlation; nonlinear behavior (circles), relayed  $H_aH_b$  correlation.

The cross-relaxation rates which could be measured accurately are, within experimental uncertainty, identical between 600 and 1000 MHz, and their mean value is reported in Table 2.

**Table 2. Experimentally Determined Cross-Relaxation Rates (or Product of Cross-Relaxation Rates in the Case of a Relayed Correlation)**

$\sigma_{H_aH_b}$ (s $^{-1}$ )	$\sigma_{H_aH_c}$ (s $^{-1}$ )	$\sigma_{H_aH_b}$ (s $^{-1}$ )	$\sigma_{H_aH_c(1)}$ (s $^{-1}$ )	$\sigma_{H_aH_c(2)}$ (s $^{-1}$ )	$\sigma_{H_aH_c} \sigma_{H_aH_b}/2$ (s $^{-2}$ )
-0.26	-0.08	-0.10	-0.07	-0.06	0.17

All cross-peaks are of the same sign as the diagonal peaks, indicating that cross-relaxation rates are negative. As a matter of fact, we shall now proceed with the ratio of a given cross-relaxation rate  $\sigma_{ij}$  to  $\sigma_{H_aH_b}$ , as is usually done,<sup>23–25</sup> and deduce an apparent distance  $r_{ij}$ . In fact,  $\sigma_{ij}$  can be expressed as  $p(\sigma_{ij})_{\text{gel}} + (1-p)(\sigma_{ij})_{\text{iso}}$ . Because  $|(\sigma_{ij})_{\text{iso}}|$  is much smaller than  $|(\sigma_{ij})_{\text{gel}}|$ ,  $\sigma_{ij}$  reduces to  $p(\sigma_{ij})_{\text{gel}}$ , and because those cross-relaxation rates are frequency independent, we can write

$$r_{ij} = 2.5 \left[ \frac{\sigma_{H_aH_b}}{\sigma_{ij}} \right]^{1/6} = 2.5 \left[ \frac{(\sigma_{H_aH_b})_{\text{gel}}}{(\sigma_{ij})_{\text{gel}}} \right]^{1/6} \quad (14)$$

$\sigma_{H_aH_b}$ ,  $\sigma_{H_aH_c(1)}$ , and  $\sigma_{H_aH_c(2)}$  do not present much interest, but as their values lie in the expected range, they validate the whole set of measurements. Conversely, let us turn to  $\sigma_{H_aH_c}$  which definitely represents a direct correlation as evidenced in Figure 10. The corresponding interatomic distance calculated according to eq 12 is 2.6 Å, while the meta H–H distance in an aromatic cycle is around 4.3 Å. Clearly, this correlation cannot be intramolecular but merely represents the dipolar interaction of  $H_a$  and  $H_c$  belonging to different molecules. This is presumably related to the so-called  $\pi$ – $\pi$  stacking and reveals the interaction between the naphthalimide moieties of two different gelator molecules which certainly has some importance in the gel formation. It must however be noted

that, due to spin diffusion within the whole naphthalimide spin system, this distance is presumably slightly approximate.

The last correlation to understand is between  $H_i$  and  $H_a$ . Obviously, due to the very large distance separating these two protons in the gelator molecule, the  $H_i$ – $H_a$  correlation cannot be intramolecular. On the other hand, it is a relayed correlation (Figure 10). This is not so surprising because it seems difficult to admit that a  $CH_2$  grouping can interact with a naphthalimide moiety. In fact, it can be noticed that the protons labeled by  $i$  in Figure 1 are close to an aromatic cycle ( $j$  in Figure 1). Again, we can invoke  $\pi$ – $\pi$  stacking and the resulting head-to-tail structure proposed<sup>8</sup> for explaining the organogel structure. Thus, as anticipated in Table 2, the intermolecular correlation between  $i$  and  $a$  implies first an intramolecular dipolar interaction between  $i$  and  $j$ , relayed by the intermolecular dipolar interaction between  $j$  and  $a$ . Estimating the distance between  $H_i$  and the ortho protons of the aromatic cycle  $j$ , it is possible to evaluate  $\rho(\sigma_{H_i H_j})_{\text{gel}}$  at  $-0.26 \text{ s}^{-1}$ . From the experimental value given in Table 2 ( $(\sigma_{H_i H_j} \sigma_{H_j H_a})/2 = \rho(\sigma_{H_i H_j})_{\text{gel}}(\sigma_{H_j H_a})_{\text{gel}}/2 = 0.17 \text{ s}^{-2}$ ), we arrive at a reasonable distance of about 2.4 Å between the aromatic cycle  $j$  and the naphthalimide  $H_a$  proton.

It must be finally mentioned that these two intermolecular correlations are absent in the NOESY spectrum (not shown) of the same system beyond the gel–liquid transition, confirming that they are specific to the organogel structure.

## CONCLUSION

Techniques associated with proton nuclear spin relaxation, which have been widely used for structural and dynamical studies of large biomolecules, have been for the first time (to the best of our knowledge) applied to low-molecular-weight organogels. It has first been demonstrated that the visible proton NMR spectrum arises from gelator molecules in fast exchange between the gel structure and the so-called isotropic compartment, which permits the observation of a high-resolution NMR spectrum. These conclusions have been reached (i) by extensive measurements of spin–lattice relaxation times (laboratory and rotating frames) as a function of temperature and (ii) by the analysis of the spin–lattice relaxation times in the rotating frame measured at low resonance frequencies in both phases (gel and liquid). This fast exchange situation allows us to derive, from the visible NMR spectrum, information about the organogel itself. In particular, from NOESY measurements, we could access not only geometrical parameters but also specific relaxation rates, both quantities pertaining to the gel structure. At the onset, the whole set of relaxation parameters leads to the characterization of gelator dynamics in the gel structure and in the isotropic compartment. This confirms the organogel flexibility and the presence of gelator clusters in the isotropic phase. Concerning geometrical determinations, we designed a test for discriminating between direct and relayed correlations, leading to the clear identification of intermolecular dipolar interactions. The latter support nicely an assumed structure of the system under investigation: columns of gelator molecules with a head-to-tail configuration and partial entanglement of these columns. Finally, it can be emphasized that the intermolecular correlations observed in organogels are reminiscent of the early elucidation of protein tertiary structure by NOESY experiments.

## ASSOCIATED CONTENT

### Supporting Information

Details of the theory about NOESY peak intensities. This material is available free of charge via the Internet at <http://pubs.acs.org>.

## AUTHOR INFORMATION

### Corresponding Author

daniel.canet@univ-lorraine.fr

### Notes

The authors declare no competing financial interest.

## ACKNOWLEDGMENTS

This work is part of the Agence Nationale de la Recherche (ANR) project MULOWA (Grant Blan08-1\_325450). Financial support from the Très Grand Equipement de Résonance Magnétique Nucléaire à Très Haut Champ (TGE RMN THC) FR3050 for conducting the research is gratefully acknowledged.

## REFERENCES

- (1) Terech, P.; Weiss, R. G. *Chem. Rev.* **1997**, *97*, 3133.
- (2) Weiss, R. G.; Terech, P. *Molecular Gels*; Springer: Dordrecht, The Netherlands, 2006.
- (3) Terech, P.; Pasquier, D.; Bordas, V.; Rossat, C. *Langmuir* **2000**, *16*, 4485.
- (4) George, M.; Weiss, R. G. *Chem. Mater.* **2003**, *15*, 2879.
- (5) Brosse, N.; Barth, D.; Jamart-Grégoire, B. *Tetrahedron Lett.* **2004**, *45*, 9521.
- (6) Pham, Q. N.; Brosse, N.; Dumas, D.; Hocquet, A.; Jamart-Grégoire, B. *New J. Chem.* **2008**, *32*, 1131.
- (7) Yemloul, M.; Steiner, E.; Robert, A.; Bouguet-Bonnet, S.; Allix, F.; Jamart-Grégoire, B.; Canet, D. *J. Phys. Chem. B* **2011**, *115*, 2511.
- (8) Allix, F.; Curcio, P.; Nghi Quoc, P.; Pickaert, G.; Jamart-Grégoire, B. *Langmuir* **2010**, *26*, 16818.
- (9) Youxing, Q.; Songping, L.; Jizhen, D.; Xiuchai, L.; Renji, Z.; Xiaocheng, G. *J. Protein Chem.* **1997**, *16*, S65.
- (10) Cavanagh, J.; J. Fairbrother, W.; Palmer, A. G.; Skelton, N. J. *Protein NMR Spectroscopy: Principles and Practice*; Academic Press: New York, 1995.
- (11) Steiner, E.; Yemloul, M.; Gueudou, L.; Leclerc, S.; Robert, A.; Canet, D. *Chem. Phys. Lett.* **2010**, *495*, 287.
- (12) Placin, F.; Colomès, M.; Desvergne, J.-P. *Tetrahedron Lett.* **1997**, *38*, 2665.
- (13) Meyer, B.; Peters, T. *Angew. Chem., Int. Ed.* **2003**, *42*, 864.
- (14) Rosevear, P. R.; Mildvan, A. S. *Methods Enzymol.* **1989**, *177*, 333.
- (15) Szyperski, T.; Luginbühl, P.; Otting, G.; Güntert, P.; Wüthrich, K. *J. Biomol. NMR* **1993**, *3*, 151.
- (16) Loria, J. P.; Berlow, R. B.; Watt, E. D. *Acc. Chem. Res.* **2008**, *41*, 214.
- (17) Akke, M.; Palmer, A. G. M. *J. Am. Chem. Soc.* **1996**, *118*, 911.
- (18) Deverell, C.; Morgan, R. E.; Strange, J. H. *Mol. Phys.* **1970**, *18*, 553.
- (19) Meiboom, S. *J. Chem. Phys.* **1961**, *34*, 375.
- (20) Solomon, I. *Phys. Rev.* **1955**, *99*, 559.
- (21) Olejniczak, R. T.; Gampe, Jr.; Fesik, S. W. *J. Magn. Reson.* **1986**, *67*, 28.
- (22) Macur, S.; Farmer, B. T.; Brown, L. R. *J. Magn. Reson.* **1986**, *70*, 493.
- (23) Jones, C. R.; Butts, C. P.; Harvey, J. N. *Beilstein J. Org. Chem.* **2011**, *7*, 145.
- (24) Neuhaus, D.; Williamson, M. P. *The Nuclear Overhauser Effect in Structural and Conformational Analysis*, 2nd ed.; John Wiley & Sons, Inc.: New York, 2000.
- (25) Butts, C. P.; Jones, C. R.; Towers, E. C.; Flynn, J. L.; Appleby, L.; Barron, N. J. *Org. Biomol. Chem.* **2011**, *9*, 177.